Research Article

A new method for detecting jittered PRI in histogram-based methods

Mostafa BAGHERI, Mohammad Hossein SEDAAGHI**
Department of Electrical Engineering, Sahand University of Technology, Tabriz, Iran

Abstract: Histogram-based methods are among the best methods for deinterleaving, because of their easy implementation. However, they have a basic defect when they encounter a jittered pulse repetition interval (PRI). Jittered PRI is one of the most sophisticated patterns for electronic warfare (EW) receivers. In jittered PRI, the time among successive pulses varies in a totally random manner; thus its detection is very complicated. In this paper we present a new method for extracting jittered PRI from histogram-based methods. Simulation results demonstrate excellent performance of the proposed method in normal as well as hard circumstances where a higher missing pulse rate occurs or even when several targets with PRI of type jitter exist.

Key words: Radar, electronic support, pulse repetition interval, deinterleaving, jittered PRI

1. Introduction

Radar reconnaissance equipment, known as electronic support measure (ESM) [1], is one of the most important parts in electronic warfare, performing threat detection and area surveillance to determine the bearing and identity surrounding radar emitters. The ESM receiver, which is passive, picks up the pulses emitted by surrounding radars in the environment and measures their five identifying parameters: angle of arrival (AOA), radio frequency (RF), pulse width (PW), pulse amplitude (PA), and time of arrival (TOA).

Very often, pulse trains from a number of different sources are received on a communication channel. On the assumption that each one of these trains has different characteristics from the others, one may be interested in sorting out pulse trains and thus identifying the source of the pulses. This task is termed deinterleaving [2].

Deinterleaving can be single-parametric [3–23] or multiple-parametric [24–27]. In multiple-parameter algorithms, two or more parameters are used for deinterleaving while in single-parameter ones, only one parameter is utilized [3]. Among all pulse parameters, TOA is of considerable interest since it leads to a key derived parameter called pulse repetition interval (PRI), which represents the difference of sequential TOAs of the received pulses [4]. Thus, methods that use TOA for deinterleaving have been the focus of many studies. In the work by Bagheri and Sedaaghi [3], an adaptive threshold was proposed to detect/extract candidate PRIs from histogram-based methods. The main idea is based on choosing a threshold in the constant false alarm rate (CFAR) receiver. In [4], Gençol et al. have introduced a new feature set for the problem of recognizing PRI modulation patterns. The recognition is based upon the features extracted from the multiresolution decomposition of different types of PRI modulated sequences. Moore and Krishnamurthy [5] have formulated the problem as a stochastic discrete-time dynamic linear model (DLM) with fixed look-ahead and probabilistic

---

*Correspondence: sedaaghi@sut.ac.ir

teacher Kalman filtering for the estimation task. In the research by Orsi et al. [6], an FFT-based method has been proposed to extract pulse repetition frequency (PRF = 1/PRI). It focuses solely on determining the number of pulse trains present and the frequency of each pulse train without actually deinterleaving them. Perkins and Coat have used the image processing technique known as Hough transform to solve the nonlinear problem of pulse train deinterleaving [7]. Conroy and Moore [8] have proposed a method to estimate the interleaved pulse train phase. Nishiguchi and Kobayashi [9] have proposed a method called modified PRI transform that is a nonlinear integral transform. It retained the peaks corresponding to PRIs and completely suppressed the peaks of the subharmonics. In 2005, Nishiguchi proposed a method called the PRI map, which is an extension of PRI transform by a time period analysis [10]. By this extension,

pulse trains become detectable even if their PRIs are jittered, and they exist for short time periods in the observation period. The usage of cumulative difference (CDIF) histograms and sequential difference (SDIF) histograms in deinterleaving has been described in [11,12]. The first CDIF consists of a histogram of the first differences of TOAs. Peaks will occur if there exist regions in the data record without any interleaving. If no peaks are found, a histogram of the second differences of the TOAs is added to the histogram of the first differences and the cumulative histogram is examined for peaks, and so on. The advantage is that a noninterleaved pulse train can be found immediately. This greatly reduces the number of differences needed to get started and may also reduce the confusion caused by multiples of the PRIs. The SDIF histogram approach makes use of the first differences of the TOAs in the same way as the first step of the CDIF approach. However, the second differences of the TOAs are used to form a separate histogram, rather than being added to the histogram of the first differences. Each higher order difference is used to form its own histogram whose peaks are then used to infer interval values in conjunction with the results from the other lower order difference histograms [13].

Since histogram-based algorithms are based only on subtractions, they are widely used in modern ESM receivers [14]. However, they have basic defect against jittered PRI [15].

Generally, radar pulse sequences have three types: constant, staggered, and jittered. The constant sequence contains a single PRI, while the staggered one has M pulse gaps, $T_1, \ldots, T_M$, that repeat in M-count cycles [15]. Jittered PRI means that there is a random deviation of the interval around a mean value (τ_c) and the deviation is homogeneously distributed [16]. Consecutive pulses are generated as follows [4]:

$$t_j = (j-1)\,\tau_c \pm \alpha\tau_c + t_\varphi; \quad j = 1, \ldots, N, \tag{1}$$

where t_j and τ_c denote TOA and the central PRI, respectively, and α is the deviation factor. Having such variations implies radar capabilities lacking in constant PRI radar. Intentional jitter is used for electronic protection (EP) from certain types of jamming and would therefore be of interest to the electronic intelligence (ELINT) analyst. Clearly, the presence of a number of intentionally jittered signals can cause problems for interval-only deinterleavers [13].

Milojevic and Popovic have introduced a threshold function in [12] to determine which histogram represents possible PRIs. Clearly, if the number of available pulses is fixed, the number of existing intervals will inversely be proportional to the length of the interval in the SDIF histogram. The impure intervals, representing the time among the pulses of different pulse trains, are personified as random Poisson points [13]. This leads to a threshold function of the form

$$p\left(\tau\right) = \delta\left(N - c\right) e^{-\tau/\rho B} \tag{2}$$

where N is the total number of pulses, B is the total number of bins, and c is the difference level, while δ and ρ are experimentally determined constants.

In fact, the deviation from the central PRI causes pulses from the jittered PRI to spread into some of the bins around the central one. Thus, the jittered PRI's peak decreases and may not be detected by the aforementioned threshold.

In this paper we propose a new method that can solve the problem of detecting jittered PRI in histogram-based methods.

The organization of the paper is as follows. Section 2 introduces the proposed method. The analyses and results of the simulations are discussed in Section 3. Finally, Section 4 concludes the paper.

2. Proposed method

Among all algorithms that have been introduced in the literature to recognize pulsed radars, histogram-based methods are widely used in modern ESM receivers [14]. However, the peaks in jittered PRI are very small in the histogram of differences and therefore their detection/extraction is very complicated. Thus, in this paper we focus on extracting jittered PRI from the histogram of differences.

2.1. Differential histogram forming

Let N interleaved pulses be recorded as [17]

$$t_i \{t_1, t_2 \ldots, t_N\} \tag{3}$$

where t_i denotes TOA of the ith pulse and $t_j > t_i > 0, \ \ \forall j > i > 0$.

All TOA differences from t_i up to c adjacent pulses are computed as follows:

$$\Delta t = t_{c+i} - t_i \tag{4}$$

c is called difference level and is increased by one until

$$t_{c+i} - t_i > PRI_{\max} \tag{5}$$

Later, the ith pulse is ignored and the process continues with other TOAs.

The time vector in the histogram is divided into B sections (also called bins). Bin's width, denoted b, is computed as

$$b = \frac{PRI_{\max} - PRI_{\min}}{B}, \tag{6}$$

where $PRI_{\max}$ and $PRI_{\min} PRI_{\max}$ denote maximum and minimum values of acceptable PRI, respectively. B is a constant indicating the number of bins. $PRI_{\min}$, $PRI_{\max}$, and B are predefined values. Finally, each Δt is placed into an appropriate bin $(\tau_1, \ldots, \tau_K)$.

2.2. Windowing

In order to extract the jittered PRI from the histogram of differences, a window is convolved with the values of bins. If two pulses are received from a radar, the difference will be a true PRI; otherwise a false one will be generated. Let us denote the former as pure interval and the latter as impure interval. Since impure intervals are

caused by the mutual interference of signal sources with different PRIs, they are not accumulated [9]. However, they constitute noise components of the histogram. Impure intervals (histogram noise) are denoted as H_n.

For radar with jittered PRI, since pulses are transmitted with deviation (i.e. $(1 \pm \alpha\%)\tau_c$), the neighboring bins around the corresponding one for τ_c will be occupied. Thus, they will fall below the threshold and cannot be detected. In order to extract the jittered PRI from the histogram, we have suggested a convolution of the form

$$y[\tau_v] = \sum_{k=\tau_v-\frac{l_w}{2}}^{\tau_v+\frac{l_w}{2}} x[k]\, w[\tau_v - k], \tag{7}$$

where $x[k]$ is the kth bin value and $w[k]$ and l_w are the window function and window length respectively. Moreover, since the amount of the deviation is not clear in advance, it should be set to the maximum acceptable value, to detect the real peak of the jittered PRI:

$$l_w[\tau_k] = \pm \alpha_{\max}\tau_k \qquad k = 1, \ldots, B \tag{8}$$

2.3. The characteristics of the selected window

Let the jittered PRI have a uniform distribution of width l ($l = \pm \alpha\tau_c$). The selected window should have the same width and distribution. The width of the window is required to be changed to fit the width of the jittered PRI, because in higher values of n the jittered PRI's peak is spread into more bins.

When the center of the window and jittered PRI overlap completely, the output, $[\tau_v]$, is equal to $A\frac{t_N}{\tau_c}$. A is a constant that depends on window type. It means that after convolution the jittered PRI's peak increases and can accurately be extracted.

However, there is a major problem when there exist two jittered PRIs in the input pulse train and their centers are close together. After convolution, the length of output is $2l$, where l is the width of the jittered PRI. On the other hand, if two jittered PRIs exist whose central PRIs have distance less than $2l$, they will produce an overlap and cannot be separated correctly. In the following we introduce a new window to overcome this problem.

2.4. Proposed window

Flat-top window is the best one among other windows to cure the above-mentioned problem. It has two side lobes with negative coefficients and a positive main lobe [28]. Each side lobe width is $l_n = 0.28l_w$ (l_w is the width of the window) and their average negative coefficients are equal to $\beta_n = -0.03$. Furthermore, the main lobe has $l_p = 0.44l_w$ and $\beta_p = 0.53$ width and average positive coefficients, respectively.

The three following cases will happen when the window is applied for convolution:

1. $|\tau_c - \tau_v| > 2\alpha\tau_c$

   It means that there is no overlap between the window and jittered PRI bins. For such window, the output becomes

   $$y[\tau_v] = 0.44l_w\beta_p\bar{\mu}_n - 2(0.28l_w\beta_n\bar{\mu}_n) \cong 0.21l_w\bar{\mu}_n \tag{9}$$

   where $\bar{\mu}_n$ is the average height of the impure intervals (H_n) given by [3]

   $$\bar{\mu}_n = \frac{1}{2}\left[\left(\sum_{d=1}^{D} n_d\right)^2 - \sum_{d=1}^{D} n_d^2\right]\frac{b}{t_N} \tag{10}$$

Here n_d is the number of pulses from each of the D pulse trains, and b and t_N are bin's width and the last time of arrival, respectively.

2. $|\tau_c - \tau_v| < 2\alpha\tau_c$

i.e. the window and jittered PRI bins have partial overlap. Thus, the output would be

$$y[\tau_v] = \sum_{k=\tau_v - \frac{l_w}{2}}^{\tau_v + \frac{l_w}{2} - \eta l - 1} x[k]\, w[\tau_v - k] + \sum_{k=\tau_v + \frac{l_w}{2} - \eta l}^{\tau_v + \frac{l_w}{2}} x[k]\, w[\tau_v - k] \tag{11}$$

where η is the overlap coefficient derived by

$$\eta = \frac{2\alpha\tau_c - (|\tau_c - \tau_v|)}{2\alpha\tau_c} \tag{12}$$

When there is partial overlap among the window and jittered PRI bins, the output increases/decreases gradually when the overlap coefficient is equal to one/zero. When $\eta = 0$, there is no overlap and the output should have the value of (8). Moreover, when $\eta = 1$, the window and jittered PRI bins completely overlap, which will be discussed in the following section.

3. $|\tau_c - \tau_v| = 0$

In this case the window and jittered PRI bins overlap completely. Therefore, the output becomes maximum:

$$y[\tau_v] = 0.44 l_w \beta_p \bar{\mu}_j - 2\left(0.28 l_w \beta_n \bar{\mu}_j\right) \cong 0.21 l_w \bar{\mu}_j \tag{13}$$

Here $\bar{\mu}_j$ is the mean peak of the jittered PRI:

$$\bar{\mu}_j = \left(\frac{T_N}{l\tau_c}\right) + \bar{\mu}_n \tag{14}$$

As a result,

$$y[\tau_v] = 0.21\left(\frac{T_N}{\tau_c} + l_w \bar{\mu}_n\right) \tag{15}$$

After convolution and eliminating the negative parts of the output, the output's width becomes

$$L_{out} = l_w + l - 2\left(0.28 l_w\right) = l + 0.44 l_w \cong 1.44 l \tag{16}$$

That is less than the output's width generated by other windows. Therefore, it improves the resolution. However, the applied window has two main defects:

(a) When there is no overlap (case 1), the output is related to the window's width (l_w). Therefore, in higher bins (where the window occupies more bins), the output value increases gradually even when there is no PRI. In fact, the window magnifies histogram noise (H_n) and it may cause false alarms.

(b) The average coefficients of the window are about 0.21. It means that the detected PRI is about 21% of the real peak (refer to (13)) and so it might fail to detect the jittered PRI, especially when the missing pulses rate is high.

Hence, a new window needs to be introduced to improve the performance. The suggested window is derived as

$$
w[n] = \begin{cases} -1 & -2\alpha n \leq n \leq -\alpha n \\ 1 & -\alpha n + 1 \leq n \leq \alpha n \\ -1 & \alpha n + 1 \leq n \leq 2\alpha n \\ 0 & \text{otherwise} \end{cases}
\tag{17}
$$

Five cases with the new window occur:

1. $|\tau_c - \tau_v| \geq 3\alpha\tau_c$

   In this case there is no overlap among the window and jittered PRI bins; thus,

   $$
   y[\tau_v] = -\alpha\tau_v\bar{\mu}_n + 2\alpha\tau_v\bar{\mu}_n - \alpha\tau_v\bar{\mu}_n = 0
   \tag{18}
   $$

2. $2\alpha\tau_c \leq |\tau_c - \tau_v| < 3\alpha\tau_c$

   In this case, one of the negative parts of the window partially overlaps with the jittered PRI:

   $$
   \begin{aligned}
   y[\tau_v] &= -\alpha\tau_v\bar{\mu}_n + 2\alpha\tau_v\bar{\mu}_n - (1-\eta)\alpha\tau_v\bar{\mu}_n - \eta\alpha\tau_v\bar{\mu}_j \\
   &= \eta\alpha\tau_v\left(\bar{\mu}_n - \bar{\mu}_j\right),
   \end{aligned}
   \tag{19}
   $$

   where η is the overlapping factor computed as

   $$
   \eta = \frac{3\alpha\tau_c - (|\tau_c - \tau_v|)}{\alpha\tau_c}
   \tag{20}
   $$

   η is always between $(0,1]$, and substituting (14) into (19), the output will be

   $$
   -\frac{T_N\tau_v}{2\tau_c^2} \leq y\left(\tau_v\right) < 0
   \tag{21}
   $$

3. $\alpha\tau_c \leq |\tau_c - \tau_v| < 2\alpha\tau_c$

   In this case, jittered PRI bins and one of the negative parts of the window will completely overlap but the positive part of the window will imbricate partially. Thus:

   $$
   \begin{aligned}
   y[\tau_v] &= -\alpha\tau_v\bar{\mu}_n + \alpha\tau_v\bar{\mu}_n + \eta\alpha\tau_v\bar{\mu}_j + (1-\eta)\,\alpha\tau_v\bar{\mu}_n - \alpha\tau_v\bar{\mu}_j \\
   &= (1-\eta)\,\alpha\tau_v\bar{\mu}_n + (\eta-1)\,\alpha\tau_v\bar{\mu}_j,
   \end{aligned}
   \tag{22}
   $$

   where

   $$
   \eta = \frac{2\alpha\tau_c - (|\tau_c - \tau_v|)}{\alpha\tau_c}
   \tag{23}
   $$

   and hence

   $$
   -\frac{T_N\tau_v}{2\tau_c^2} < y\left(\tau_v\right) \leq 0
   \tag{24}
   $$

4. $\alpha\tau_c \leq |\tau_c - \tau_v| < 0$

   When one of the negative and positive parts of the window partially overlaps with the jittered PRI bins, we have

   $$y[\tau_v] = -\alpha\tau_v\bar{\mu}_n + (1 - \eta)\,\alpha\tau_v\bar{\mu}_n + (1 + \eta)\,\alpha\tau_v\bar{\mu}_j - (1 - \eta)\alpha\tau_v\bar{\mu}_j - \eta\alpha\tau_v\bar{\mu}_n, \tag{25}$$

   where

   $$\eta = \frac{\alpha\tau_c - (|\tau_c - \tau_v|)}{\alpha\tau_c} \tag{26}$$

   Therefore,

   $$0 < y(\tau_v) < \frac{T_N\tau_v}{\tau_c^2} \tag{27}$$

5. $\tau_c - \tau_v = 0$

   In this case, the window and jittered PRI bins are overlapped completely. Thus

   $$y(\tau_v) = -\alpha\tau_c\bar{\mu}_n + 2\alpha\tau_c\bar{\mu}_j - \alpha\tau_c\bar{\mu}_n = \frac{T_N}{\tau_c} \tag{28}$$

The proposed window has two great advantages:

(a) The average positive coefficients are 1. Thus, it can detect the real jittered PRI peak.

(b) The total average coefficients are zero. It means that the proposed window does not amplify noise (H_n); therefore the probability of false alarms becomes very low.

The parts discussed above are demonstrated in Figure 1.
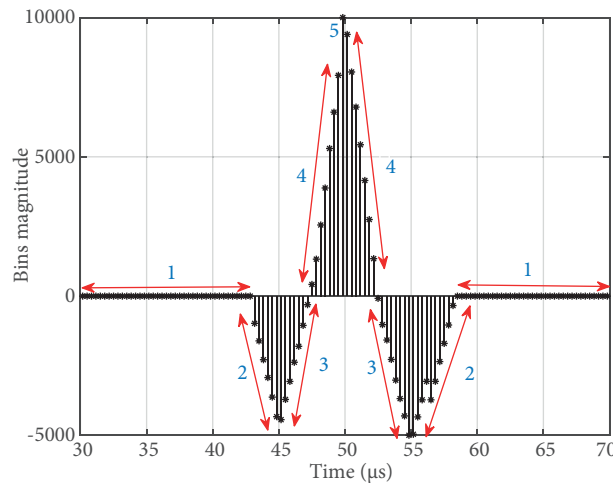
Figure 1. Five parts of the output generated by proposed window.

By eliminating the negative parts of Figure 1, the output's length will be

$$L_{out} = 6\alpha\tau_c - 4\alpha\tau_c = 2\alpha\tau_c = l \tag{29}$$

It means that the output's length and jittered PRI's length are the same. Thus, the resolution of the proposed window is better than that of other windows.

3. Simulation and analysis

In this section, the proposed method is simulated. The convolution between the flat-top window and jittered PRI bins is also presented as an accuracy comparison.

Note that for SDIF an optimal detection threshold function is derived as (2) [12]. In our simulations, we set $(\delta\rho) = (0.35, 0.6)$.

3.1. Multiple jittered PRIs

Let the received pulses be the combination of two jittered PRIs. Their specification is given in Table 1. In our example, the total number of pulses and missing pulse rate are 10,000 and 25%, respectively.

Table 1. Jittered PRIs' specifications.

Jittered PRI	$\tau_c(\mu s)$	$\alpha\%$
PRI$_1$	83	10% ($\pm$5%)
PRI$_2$	95	10% ($\pm$5%)

Simulation results are depicted in Figure 2. Figure 2a shows the histogram of differences. Figure 2b demonstrates that the flat-top window fails to detect the PRIs. Moreover, histogram noise is gradually amplified by increasing the length of the window. It will produce false alarms. However, the proposed window successfully detects all PRIs without amplifying H_n (Figure 2c).
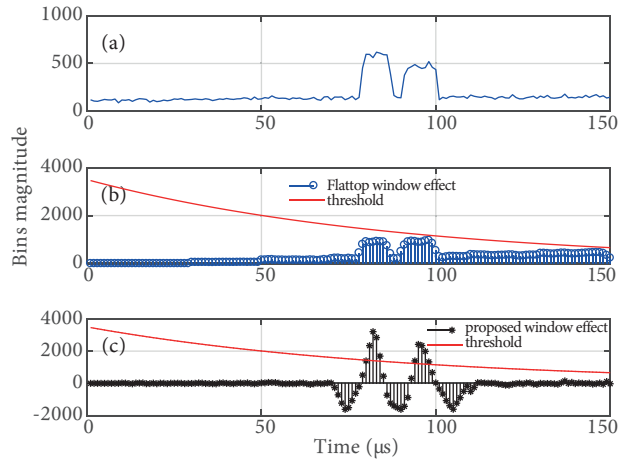
Figure 2. a. Histogram of differences, output by b. flat-top window, c. the proposed window.

Figure 3 shows the detection capability of the proposed method versus different missing pulse rates. As can be seen, when the number of jittered PRI increases, the detection rate decreases. That is because the ratio of pure to impure intervals decreases as the number of interleaved pulse trains increases [13]. The result is obtained by 100 Monte Carlo trials while the detection rate is derived by

$$\frac{1}{M}\sum_{i=1}^{M}\frac{D_i}{K}, \tag{30}$$

where M is the number of Monte Carlo trials, and D_i and K are the number of correct detection in ith iteration and number of jittered PRI, respectively.
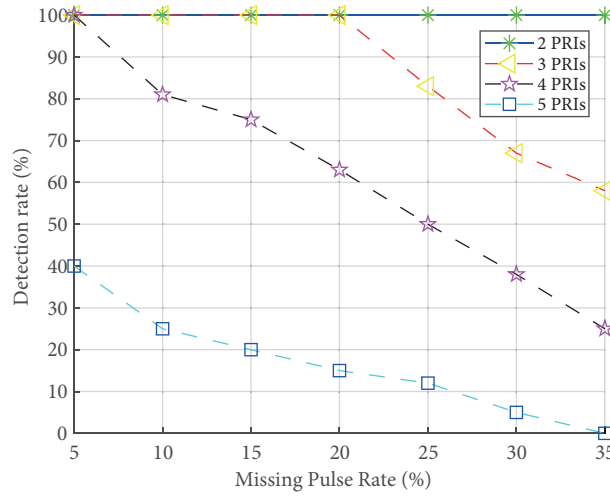
Figure 3. Detection probability vs. missing pulse rates in different number of jittered PRIs.

Table 2 summarizes the comparison among the efficiency of different window types in three categories:

Table 2. PRI specifications of radars in mixed signals case.

	φ	ν	Ω
Hanning	$2l$	50%	$0.5 \; lH_n$
Blackman	$2l$	42%	$0.42 \; lH_n$
Flat-top	$1.44l$	21%	$0.21 \; lH_n$
Proposed window	l	100%	0

1. Resolution (φ): which indicates the minimum acceptable distance between the centers of two jittered PRIs to be extracted correctly.

2. Real peak detection (ν): which pinpoints the ability of window to detect the real peak of a jittered PRI. It affects the probability of detection.

3. Noise amplification (Ω): pointing out the amplification of H_n. It predicts the probability of false alarms.

Referring to Table 2, the proposed window outperforms the others from the resolution point of view. Thus, it can separate jittered PRIs residing closely. In addition, our method can detect almost the real peak of jittered PRI, and so its probability of detection is greater than that of other windows. Therefore, it improves the detection probability in the presence of high missing pulse rates. Finally, our method does not amplify noise (H_n); on the other hand, the probability of false alarms with the proposed window is much smaller than that of others.

3.2. Special case

In section 2.2, the deviation rate was set to the largest possible value, but what happens if it is set to less than $\alpha_{\max}$? Suppose that there is a jittered PRI with $\tau_c = 100 \; \mu$s and $\alpha = 5\%$. Figure 4a shows the histogram of

differences of the mentioned scenario. The result of the convolution with the proposed window ($l_w = 10\% \, \tau_c$) is shown in Figure 4b. As can be seen, since the width of the window is larger than the jittered PRI, the peak related to the jittered PRI gets flat but is extracted correctly.
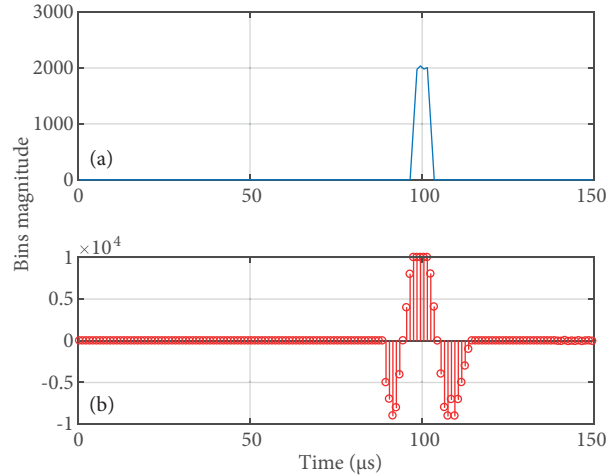
Figure 4. a. Histogram of differences, b. convolution's result by the proposed window, when the deviation rate is less than $\alpha_{\max}$.

4. Conclusion

In this paper, we have proposed a new method based on convolution to extract jittered PRI from the histogram of differences. Our method has three great advantages in high resolution, peak detection, and low false alarm rate. The first one helps to detect jittered PRIs with closer centers. The second property is employed to detect/extract this type of PRIs even in the presence of higher missing pulse rates. Finally, since it does not amplify noise, the false alarms of the proposed window are less than those of the other windows.

References

[1] Schleher D. Introduction to Electronic Warfare. Norwood, MA, USA: Artech House, 1986.

[2] Tavora R, Zubelli JP, Mattoso MA, Pinto EL. An algorithm for deinterleaving pulse trains using the fast wavelet packet transform. In: Brazilian Symposium of Telecommunications; 25–27 January 1997; Recife, Brazil, pp. 1-14.

[3] Bagheri M, Sedaaghi MH. A new approach to pulse deinterleaving based on adaptive thresholding. Turk J Elec Eng & Comp Sci 2017; 25: 3827-3838.

[4] Gençol K, At N, Kara A. A wavelet-based feature set for recognizing pulse repetition interval modulation patterns. Turk J Elec Eng & Comp Sci 2016; 24: 3078-3090.

[5] Moore JB, Krishnamurthy V. Deinterleaving pulse trains using discrete-time stochastic dynamic-linear models. IEEE T Signal Process 1994; 42: 3092-3103.

[6] Orsi RJ, Moore JB, Mahony RE. Spectrum estimation of interleaved pulse trains. IEEE T Signal Process 1999; 47:1646-1653.

[7] Perkins J, Coat I. Pulse train deinterleaving via the Hough transform. In: IEEE International Conference on Acoustics, Speech and Signal Processing; 19–22 April 1994; Adelaide, South Australia. New York, NY, USA: IEEE. pp. 1-4.

[8] Conroy TL, Moore JB. On the estimation of interleaved pulse train phases. IEEE T Signal Process 2000; 48: 3420-3425.

[9] Nishiguchi K, Kobayashi M. Improved algorithm for estimating pulse repetition intervals. IEEE T Aero Elec Syst 2000; 36: 407-421.

[10] Nishiguchi K. Time-period analysis for pulse train deinterleaving. T SICE 2005; 4: 68-78.

[11] Mardia HK. New techniques for deinterleaving repetition sequences. P IEEE Part F 1989; 136: 149-154.

[12] Milojevic DJ, Popovic BM. Improved algorithm for the deinterleaving of radar pulses. P IEEE Part F 1992; 139: 98-104.

[13] Richard G. Wiley. ELINT, the Interception and Analysis of Radar Signals. Boston, MA, USA: Artech House, 2006.

[14] Rogers JAV. ESM processor system for high pulse density radar environments. P IEE Part F 1985; 132: 621-624.

[15] Driscoll DE, Howard SD. The detection radar pulse sequences by means of a continuous wavelet transform. In: IEEE International Conference on Acoustics, Speech and Signal Processing; 15–19 March 1999; Adelaide, South Australia. New York, NY, USA: IEEE. pp. 1389-1392.

[16] Liu J, Meng H, Liu Y, Wang X. Deinterleaving pulse trains in unconventional circumstances using multiple hypothesis tracking algorithm. J Signal Process 2010; 90: 2581-2593.

[17] Kuang Y, Shi Q, Chen Q, Yun L, Long K. A simple way to deinterleave repetitive pulse sequences. In: 7th WSEAS International Conference on Mathematical Methods and Computational Techniques in Electrical Engineering; 27–29 October 2005; Sofia, Bulgaria: pp. 218-222.

[18] Ching SS, Chin TL. A vector neural network for emitter identification. IEEE T Antenn Propag 2002; 50: 1120-1127.

[19] Noone G. Radar pulse train parameter and tracking using neural networks. In: International Conference on Artificial Neural Networks and Expert Systems; 20–23 November 1995; Dunedin, New Zealand. New York, NY, USA: IEEE. pp. 95-98.

[20] Conroy TL, Moore JB. The limits of extended Kalman filtering for pulse train deinterleaving. IEEE T Signal Process 1998; 46: 3326-3332.

[21] Logothetis A, Krishnamurthy V. An interval amplitude algorithm for deinterleaving stochastic pulse train sources. IEEE T Signal Process 1998; 46: 1344-1350.

[22] Fan F, Yin X. Improved method for deinterleaving radar pulse trains with stagger PRI from dense pulse series. In: 2nd International Conference on Signal Processing Systems; 5–7 July 2010; Dalian, China. New York, NY, USA: IEEE. pp. 250-253.

[23] Ray PS. A novel pulse TOA analysis technique for radar identification. IEEE T Aero Elec Syst 1998; 34: 716-721.

[24] Guo Q, Qu Z, Wang C. Pulse-to-pulse periodic signal sorting features and feature extraction in radar emitter pulse sequences. J Syst Eng Elec 2010; 21: 382-389.

[25] He A, Zeng D, Wang J, Tang B. Multi-parameter signal sorting algorithm based on dynamic distance clustering. J Elec Sci & Tech 2009; 7: 249-253.

[26] Li H, Chen B, Han J, Dong W. A new method for sorting radiating-source. In: International Conference on Networks Security, Wireless Communications and Trusted Computing; 25–26 April 2009; Wuhan, China. New York, NY, USA: IEEE. pp. 817-819.

[27] Lin S, Thompson M, Davezac S, Sciortino JC. Comparison of time of arrival vs. multiple parameter based radar pulse train deinterleavers. J Signal Process, Sens Fusion, Target Recog 2006; 6235: 250-264.

[28] Gade S, Herlufsen H. Use of weighting functions in DFT/FFT analysis (part I). Brüel & Kjær Technical Review 1987; 3: 1-28.